Organosilane Grafted Silica: Linear Correlation of Microscopic Surface Characters and Macroscopic Surface Properties

Tuo Ji,[a] Chi Ma[b], Logan Brisbin,[a] Liwen Mu,[a] Christopher G. Robertson,[c] Yalin Dong[b] and Jiahua Zhu[a]*

[a] Intelligent Composites Laboratory, Department of Chemical and Biomolecular Engineering, The University of Akron, Akron, OH 44325 USA

[b] Department of Mechanical Engineering. The University of Akron, Akron, OH 44325 USA

[c] Eastman Chemical Company, Tire Additives Center of Excellence, Akron, OH 44333 USA

∗Corresponding author E-mail: jzhu1@uakron.edu

ABSTRACT

In polymers we see that organosilane is necessary to modify silica nanoparticles to improve their reinforcement. Properties of the modified silica surface depend on the molecular structure of silane, grafting density and consequent surface energy. Achieving maximum interfacial bonding between the filler and polymer requires precise control of silica surface property. In this work, four silanes with similar molecular structure but different alkyl chain lengths, trimethoxy(propyl)silane, trimethoxy(octyl)silane, hexadecyltrimethoxysilane and trimethoxy(octadecyl)silane, are selected as model agents to study their roles in influencing silica surface property. The grafting density of each silane on silica is well controlled by regulating the reaction conditions. Three main surface characters, silane grafting density, surface energy and surface potential, are characterized. More importantly, linear relationship has been found in grafting density vs. surface energy and grafting density vs. surface potential. Utilizing these relationships, a linear model has been developed to predict grafting density and surface energy by simply measuring surface potential. This model has been validated by additional experimental results.

Keywords: Silica, silane grafting density, surface energy, surface potential, prediction

1. Introduction

Surface functionalization of silica nanoparticles has become a prerequisite for its numerous successful applications, such as drug delivery, heterogeneous catalyst support, reinforcing filler and *etc*.[1, 2, 3, 4, 5, 6] Organosilane, abbreviated as silane in this work, is the most widely used chemical agent for silica surface modification. Silane molecules are typically comprised of two functional parts with one reactive to silica surface to form covalent bonding and the other forms physical/chemical interactions with surrounding materials. The miscellaneous option of the chemical groups in silane, including alkyl chain length, terminal functional group species and number of reactive sites,[7] provides a great platform to design silica surface functionalities. For instance, bis(triethoxysilylpropyl) tetrasulfane can enhance the dispersion and compatibility of silica nanoparticles in the poly(2,6-dimethyl-1,4-phenylene oxide) (PPO) dense membrane, which affects methanol diffusion selectivity in the liquid.[8] Also, it is possible to design nanoparticles with high stability or superhydrophobic properties.[9, 10] Indeed, the silane molecule structure determines the subsequent surface property to a great extent, while it is not the only factor since silane patterning and surface coverage govern surface properties in most cases.[7, 11] Therefore, silane molecular structure and surface coverage are equally important to achieve desired surface properties for versatile applications.

The determination of interfacial bonding and quantification of silane grafting density have been studied by using different characterization techniques.[12, 13, 14] For example, nuclear magnetic resonance (NMR) and flourier transform infrared (FT-IR)

are very useful qualitative tools to identify covalent bond formation, surface group species and cross-linking.[14, 15] To further quantify the amount of grafted molecules, thermogravimetric analysis (TGA), X-ray photoelectron spectroscopy (XPS), and atomic force microscopy (AFM) need to be used to provide specific surface information on loading, atomic ratio of different elements, and grafting coverage, respectively.[12, 16, 17, 18] A microscopic understanding of silane function requires a precise quantification of silane grafting density (or named coverage) on silica surface. Generally, only partial surface property can be accessed by using single characterization technique, which provides limited information to correlate the macroscopic surface property. Therefore, tremendous research efforts have been devoted to obtain quantitative information on surface functional groups by combining different techniques.[19] For example, Fischer et al. found the relationship between fluorescence and XPS signals, which allows a direct linkage between fluorescence analysis and XPS quantification.[16] However, it met significant challenges to quantify the grafting density of silane without nitrogen element such as silanes with aliphatic chains.[20] M. Rostami et al. utilized tensile strain experiments and dynamic mechanical thermal analysis to provide information on interfacial adhesion. By controlling the loading of silane-treated silica, it was shown that interfacial interactions was directly proportional to the amino silane content on nanosilica.[21] Those above mentioned methods require lengthy sample preparation and skillful operation of expensive instruments, which greatly restricts their usage in practical application.

Besides abovementioned techniques, some other macroscopic surface properties,

such as surface potential, wettability and surface energy[22, 23] can be used to quickly index the surface property as well. However, a quantitative correlation between molecular level information and macroscopic surface property is not available right now. Once a mathematical model between microscopic surface information and macroscopic surface property can be built, the microscopic information can be directly speculated by macroscopic surface property without involving lengthy sample preparation and expensive instrumental analysis.

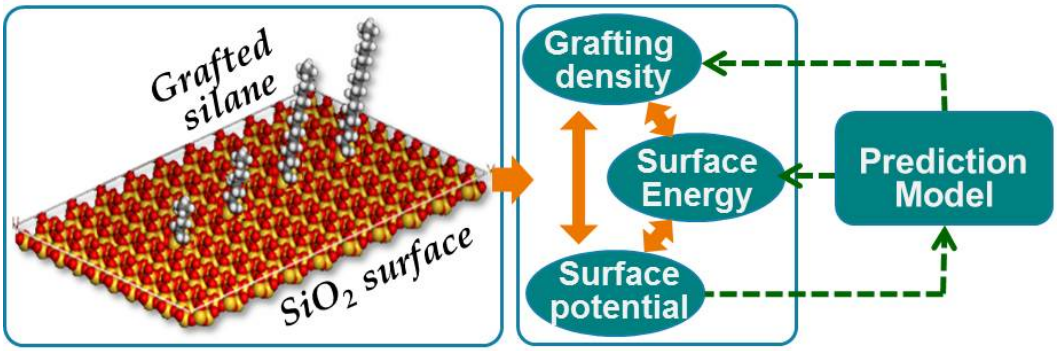

Scheme 1. Schematic diagram of the scope of this work.

In this work, we selected four different silanes with similar molecular structure but different alkyl chain lengths to modify the silica surface. By controlling the silane grafting density in a wide range, different surface properties including surface energy and surface potential can be obtained. The relationship among silane grafting density, surface energy and surface potential on each silane and across the four different silanes are explored as shown in Scheme 1. An extrapolation model is built and validated to predict the silane grafting density and silica surface energy from zeta potential. Comparing with conventional quantification methods, like NMR, XPS and TGA, this method provides obvious advantages such as convenient sample preparation and short testing time of a few minutes.

2. Experimental

2.1 Materials

Trimethoxy(propyl)silane (TMPS, $C_6H_{16}O_4Si$, 97%), Trimethoxy(octyl)silane (TMOS, $C_{11}H_{26}O_3Si$, 96%), Hexadecyltrimethoxysilane (HDTMS, $C_{19}H_{42}O_3Si$, 85%), Trimethoxy(octadecyl)silane (OTMS, $C_{21}H_{48}O_3Si$, 90%), methanol (≥99.8%) and silica powder (99.8% nanoparticle) were purchased from Sigma Aldrich. Formic acid (97%) was purchased from Acros Organics. The structural and compositional information of silane molecules are provided in Table 1. All chemicals were used as received without further purification. Deionized water (Millipore) was used throughout the experiment.

Table 1. Detailed information of silanes used in this work.

Silane	Structure	Molecular formula	Mw ($g \cdot mol^{-1}$)	$r_{a/s}$
TMPS	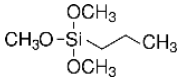	$C_6H_{16}O_4Si$	164.27	0.262
TMOS	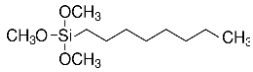	$C_{11}H_{26}O_3Si$	234.41	0.482
HDTMS	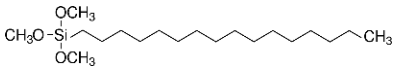	$C_{19}H_{42}O_3Si$	346.62	0.649
OTMS	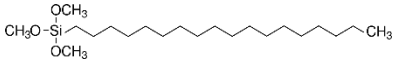	$C_{21}H_{48}O_3Si$	374.67	0.675

$r_{a/s}$: molecular weight ratio of alkyl chain to whole silane molecule.

2.2 Silica surface modification by silanes

One unit of silane was sonicated in 10.0 g of methanol:water (90:10) for 10 min and 1.0 g of formic acid was added to the mixture solution. The ratio of silane/silica is 0.5, 1.0, 2.0, 3.0 and 4.0 mol%. After 30-minute hydrolysis, 0.5 g of silica powder was

added to silane solution and then reacted at 65 ^{o}C for 24 h. The resulting samples were separated and methanol was used to rinse the samples for 3 times. The samples were then dried at 80 ^{o}C for 12 hour. The dried samples were named in the format of "silane-#". TMPS, TMOS, HDTMS and OTMS represent the four selected silanes. And # equals to 1, 2, 3, 4 and 5 for samples prepared from the silane mole percentage of 0.5, 1.0, 2.0, 3.0 and 4.0 mol%, respectively. For example, TMPS-1, TMPS-2, TMPS-3, TMPS-4 and TMPS-5 were named for silica samples grafted by TMPS with increasing silane mole percentage.

2.3 Characterization

The morphology of pure silica nanoparticle was characterized by a transmission electron microscopy (FEI Scanning TEM). Sample for TEM characterization was prepared by drying a drop of sample powder ethanol suspension on carbon-coated copper TEM grids. Brunaure–Emmet–Teller (BET) surface area analysis of silica was performed using a TriStar II 3020 surface analyzer (Micromeritics Instrument Corp., USA) with N_2 adsorption–desorption isotherms at 77 K. Fourier transform infrared (FT-IR) spectra were recorded with a Digilab Excalibur FTS 3000 series FT-IR Spectrometer using KBr pellets. The silane loading was determined by thermogravimetric analysis (TGA, TA instrument Q500) in atmospheric air from 20 to 700 ºC with a heating rate of 10 ºC/min. Contact angle images of silica and silane-grafted silica were collected by Rame-hart image system. At least eight liquid drops (2 μL for both water and ethylene glycol) on each sample were recorded for the static contact angle (CA) measurement and the average value was reported. Zeta-potential

measurements were performed in a Malvern Fetasizer Nano ZS apparatus (Malvern, UK) at 25 ^{o}C by using 0.1 wt% silica suspension.

3. Result and Discussion

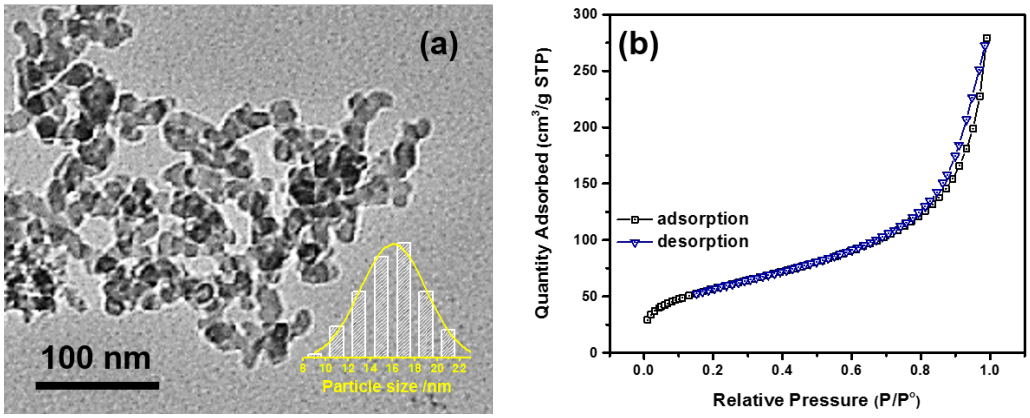

Fig.1. (a) TEM image of silica and (b) N_2 adsorption–desorption isotherms.

The morphology and surface area of the pure silica nanoparticles were characterized by TEM and BET, Fig. 1. The average diameter of silica nanoparticles is 16 nm with narrow size distribution in the range of 8-22 nm, Fig. 1(a). The statistic size distribution is based on a sampling size of >300. Nitrogen adsorption-desorption isotherms were conducted at 77 K to characterize the pore structure and surface area of the silica particle, Fig. 1(b). The major adsorption occurred at higher relative pressure ($0.6< p/p_0<1.0$) and a slender hysteresis loop was observed. The shape of the curves belongs to the type IV isotherm with a H_1 hysteresis loop, which indicates the presence of mesoporous structure.[24, 25] Looking at the aggregation structure of the silica particles in Fig. 1(a), it is not difficult to understand the existence of agglomeration induced mesoporous structure in silica. According to the multi-point BET method, the surface area of the silica particle is calculated as 199.0 m²/g.

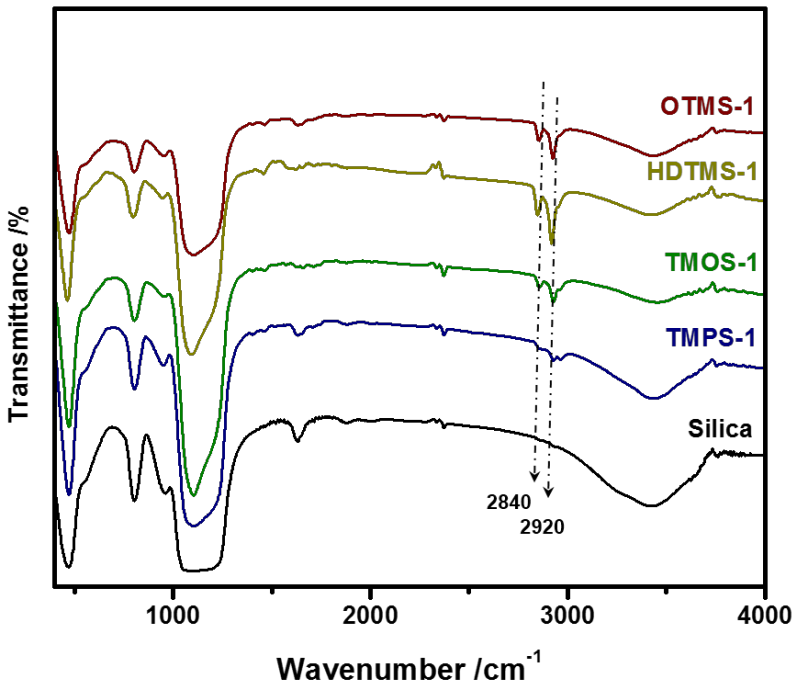

Fig. 2. FT-IR spectrum of silica and silane grafted silica particles.

In order to confirm that each kind of silane molecule is successfully grafted on the silica surface, FT-IR spectrum was performed on both silica and silane-modified silica samples, Fig. 2. The band intensity of the pure silica at 480, 803, 947 and 1100 cm^{-1} corresponds to the O-Si-O deformation, SiO_4 tetrahedron ring, Si-OH stretching and asymmetrical Si-O-Si stretching, respectively.[26] Besides these characteristic vibration bands from SiO_2, two additional CH_2 absorption bands at 2944 cm^{-1} (asymmetric stretching) and 2878 cm^{-1} (symmetric stretching) were observed in silane-modified silica. These CH_2 adsorption bands are attributed to the alkyl chain of silane molecules grafted onto the silica surface.[2, 27] Therefore, the presence of these CH_2 adsorption bands from FT-IR spectrum confirms that all the 4 silanes are successfully grafted on the silica surface.

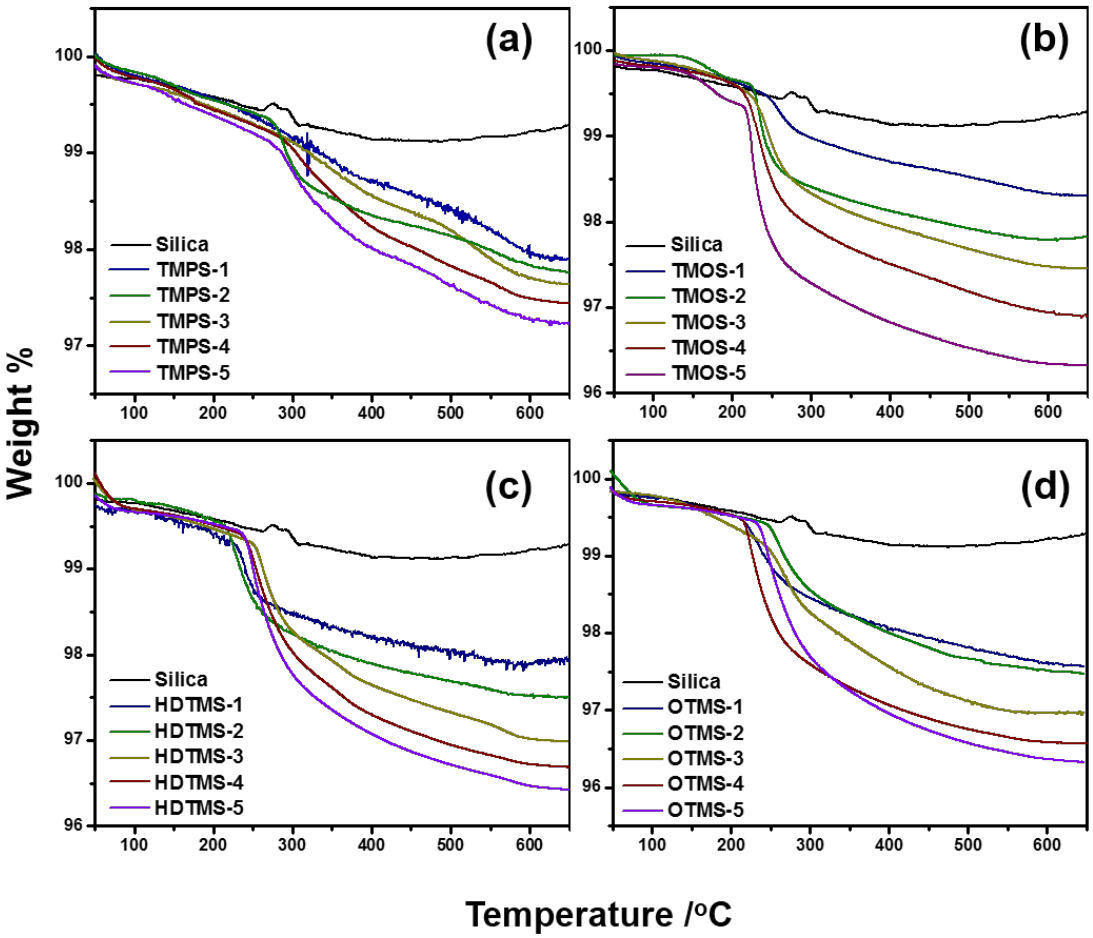

Fig. 3. TGA results of silica particles grafted by (a) TMPS, (b) TMOS, (c) HDTMS and (d) OTMS of different loadings.

The mass fraction of the volatile alkyl chain with regard to the total mass of each silane-modified silica is measured by TGA in ambient air up to 700 °C. For unmodified silica, the weight loss was observed between 40 and 200 °C, which is due to desorption of physisorbed impurities and water.[11] The second stage weight loss was from 200 to 650 °C due to the condensation of water from the hydroxyl groups at high temperature.[28] For silica modified with silane the weight loss before 200 °C was similar to that of the pure silica samples. However, from 200 to 650 °C, a more significant weight loss occurred, which is due to the decomposition of the alkyl chain in silane grafted on the silica surface.[17, 29] It is assumed that all alkyl chains of silane were removed and the rest

of the siloxy groups stay on the surface. Then, the grafted silane molar percentage (M_s%) on silica can be calculated by following equation (1):

$$M_s\% = 1/(1 + \frac{Mw_{silane}}{Mw_{silica}} \cdot (\frac{r_{a/s}}{\Delta m} - 1)) \quad (1)$$

where Mw_{silane} and Mw_{silica} are the molecular weight of silane and silica, respectively, Δm is the weight loss that occurred between 200 to 650 ^{o}C from the TGA results, $r_{a/s}$ is defined as the molecular weight ratio of the alkyl chain versus the whole silane molecule. For instance, the Δm of TMPS-1 is 1.09% after subtracting 0.8% of the weight loss occurred to pure silica. The $r_{a/s}$ is 0.26 and Mw_{silane} is 164.27 for TMPS. According to equation (1), the actual TMPS molar percentage is calculated as 1.5% for TMPS-1. Taking consideration of the measured silica surface area of 199.0 m^2/g, the silane grafting density can be further calculated as 0.79/nm^2. Theoretical calculation by Material Studio reveals the cross-section area of 0.32 nm^2 for TMPS, TMOS, HDTMS and OTMS. Based on the assumption of single layer grafting and vertical alignment of each TMPS molecule on silica surface, the silane surface coverage of TMPS-1 achieves 25.2%. Following this methodology, the actual surface coverage and grafting density of silanes in each sample are listed in Table 2.

Table 2. Summary of surface silanes in each modified silica.

	ΔM(%)	M_s(%)	D_c(%)	Ns /nm^2
TMPS-1	1.09	1.56	25.20	0.79
TMPS-2	1.30	1.88	30.22	0.94
TMPS-3	1.57	2.28	36.74	1.15
TMPS-4	1.71	2.49	40.16	1.26
TMPS-5	2.04	3.00	48.31	1.51
TMOS-1	1.53	0.39	6.32	0.20
TMOS-2	2.10	0.71	11.36	0.36
TMOS-3	2.43	0.89	14.32	0.45
TMOS-4	2.93	1.17	18.87	0.59
TMOS-5	3.60	1.56	25.07	0.78
HDTMS-1	1.78	0.26	4.27	0.13
HDTMS-2	2.28	0.40	6.49	0.20
HDTMS-3	2.71	0.52	8.42	0.26
HDTMS-4	3.03	0.61	9.87	0.31
HDTMS-5	3.19	0.66	10.61	0.33
OTMS-1	2.21	0.34	5.49	0.17
OTMS-2	2.42	0.39	6.33	0.20
OTMS-3	2.86	0.50	8.09	0.25
OTMS-4	3.28	0.61	9.79	0.31
OTMS-5	3.50	0.66	10.69	0.33

Ms: molar ratio, Dc: degree of coverage, Ns: silane number per nm^2.

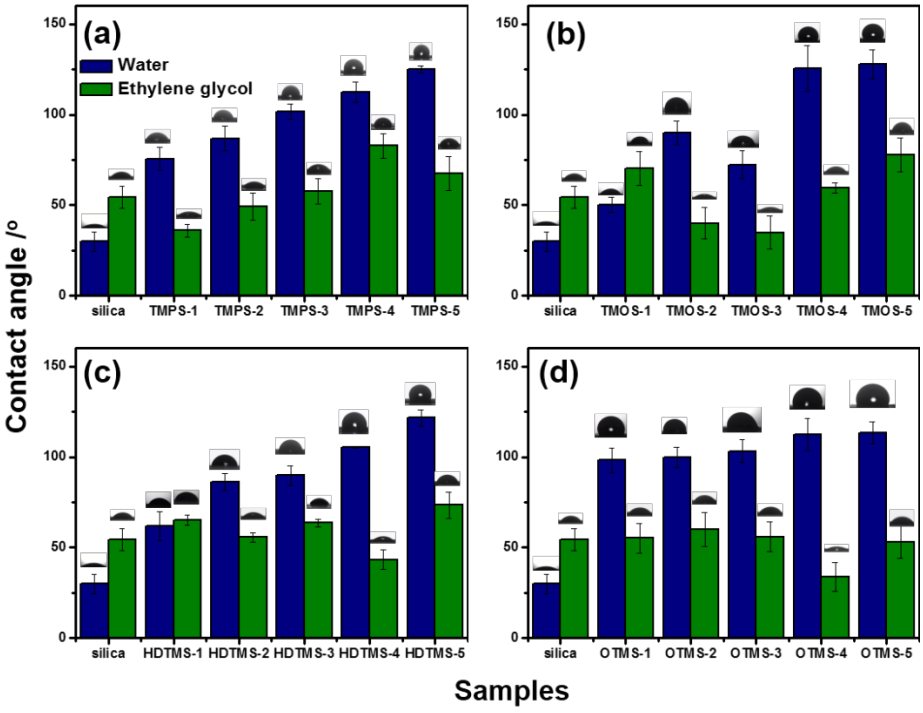

Fig. 4. Contact angle of water and ethylene glycol on silica particles grafted by (a) TMPS, (b) TMOS, (c) HDTMS and (d) OTMS.

To quantify the surface energy of silica after grafting different loadings of silanes, both water and ethylene glycol were used as probing liquid to measure the CA of each sample. As shown in Fig. 4, the pure silica shows apparent hydrophilic surface with $CA_{(water)}=30^o$ and $CA_{(ethylene\ glycol)}=54^o$, respectively. After grafting silane molecules, the water contact angle of each sample increased significantly, indicating the transition of surface property from hydrophilic to hydrophobic. By applying the Owens–Wendt model,[30] both dispersive and polar contributions to the surface energy can be calculated using equation (2):

$$\gamma_L(1+\cos\theta) = 2\sqrt{\gamma_S^D \gamma_L^D} + 2\sqrt{\gamma_S^P \gamma_L^P} \quad (2)$$

where γ_L^D and γ_L^P are the dispersive component and polar component of surface energy of the liquid probe (mN /m^2). Likewise, γ_S^D and γ_S^P are the dispersive component and polar component of surface energy of the solid (J/m^2). According to the water and ethylene contact angles, the γ_S^D and γ_S^P can be calculated and the surface energy is 115.8 mN·m^{-1}. The contact angle and surface energy of all the samples are summarized in Table 3. It's obvious that the surface energy decreases with increasing silane grafting density, Fig. 5, which is the case for all the four selected silanes due to their low surface energy alkyl terminal chains. Moreover, a highly linear relationship has been found correlating the grafting density of four silanes and surface energy of modified silica with correlation factor $R^2 \geq 0.96$, linear fitting on solid circle data points in Fig. 5. In other words, the surface energy of the modified-silica is directly determined by silane surface coverage. From the linear regression equations of the four silanes, it

is not difficult to find a larger slop from the fitting line of silanes with longer alkyl chain. With similar silane grafting density on silica, longer alkyl chain in silane leads to lower surface energy. This phenomenon is consistent with previous literature reports that longer alkyl chain facilitates its patterning into more ordered structure and thus lower surface energy.[17, 31]

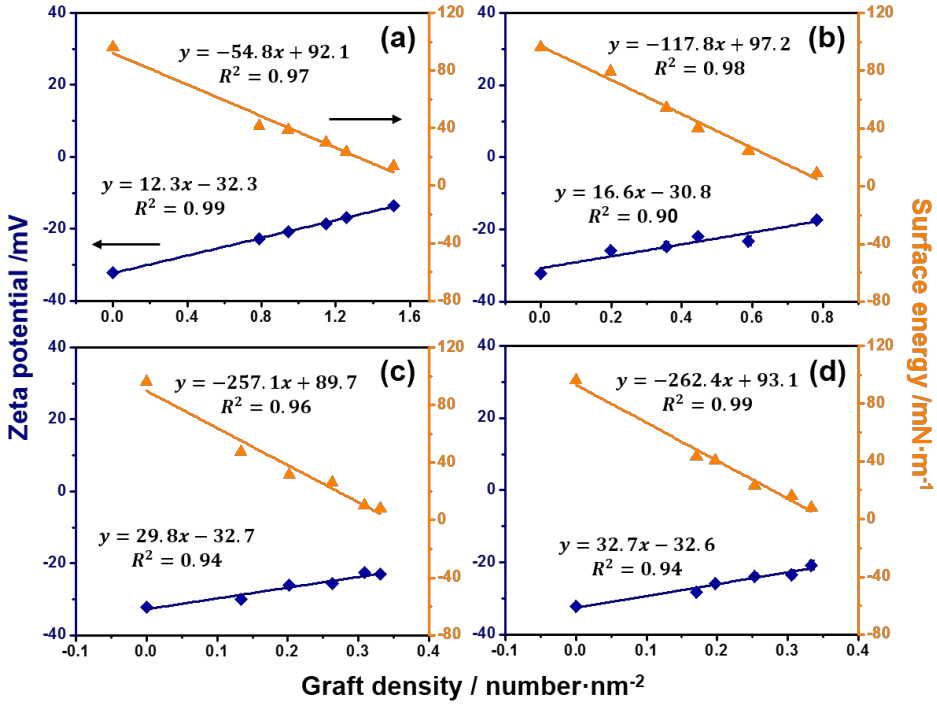

Fig. 5. Relationship of grafting density vs. zeta potential and grafting density vs. surface energy for silica grafted by (a) TMPS, (b) TMOS, (c) HDTMS and (d) OTMS.

The grafted silane on silica surface also changes its surface charge, which reflects in the change of zeta potential. According to the double-layer theory, silica nanoparticles in suspension tend to attract ions to their surface.[23] The electric potential that exists at the diffusion boundary will be affected by any surface property change on silica particles including but not limit to graft organic groups.[32, 33] The measured zeta potential of silane-modified silica is summarized in Table 3. As expected, the pure silica acquires the lowest negative potential of -32.2 mV. The zeta potential increases but

remained negative value after grafting silanes. In fact, the silica becomes less hydrophilic after grafting silanes since partial hydrophilic sites have been replaced by hydrophobic organic groups. These grafted organic groups are not able to attract ions from solution and therefore decrease the potential across the double layer. In Fig. 5 (square symbol), the surface potential demonstrates a good linear relationship with silane grafting density with correlation factor of R^2 ≥0.90. All these results reveal a good linear relationship between silane grafting density, surface energy and surface zeta potential. By acquiring one of these properties, the other two can be conveniently accessed from the linear relationship.

Table 3. Surface property of silane-modified silica particles.

	Dc **/ %**	***Ns*** **/ nm^2**	θ_{water} **/ °**	θ_{EG} **/ °**	***G*** **/ mN·m^{-1}**	***Zeta potential*** **/ mV**
Silica	0	0	30.0	54.4	96.1	-32.2
TMPS-1	25.2	0.79	75.7	36.0	41.4	-22.8
TMPS-2	30.2	0.94	86.9	49.2	38.6	-20.7
TMPS-3	36.7	1.15	101.8	57.7	30.1	-18.5
TMPS-4	40.2	1.26	112.4	82.8	23.3	-16.9
TMPS-5	48.3	1.51	125.0	67.5	13.8	-13.5
TMOS-1	6.3	0.20	50.2	70.1	79.6	-25.8
TMOS-2	11.4	0.36	90.0	40.1	54.4	-24.7
TMOS-3	14.3	0.45	72.3	35.0	40.3	-22.0
TMOS-4	18.9	0.59	125.4	59.6	24.4	-23.2
TMOS-5	25.1	0.78	127.7	77.8	8.9	-17.3
HDTMS-1	4.3	0.13	61.8	65.1	47.3	-28.4
HDTMS-2	6.5	0.20	86.3	55.7	31.4	-24.5
HDTMS-3	8.4	0.26	89.8	63.7	26.1	-22.1
HDTMS-4	9.9	0.31	105.5	43.3	10.5	-20.6
HDTMS-5	10.6	0.33	121.6	67.4	8.2	-18.5
OTMS-1	5.5	0.17	98.2	55.3	43.4	-28.2
OTMS-2	6.3	0.20	99.6	60.0	40.7	-25.8
OTMS-3	8.1	0.25	103.2	56.0	23.0	-23.9
OTMS-4	9.8	0.31	112.6	33.8	16.0	-23.4
OTMS-5	10.7	0.33	113.5	52.8	7.9	-20.7

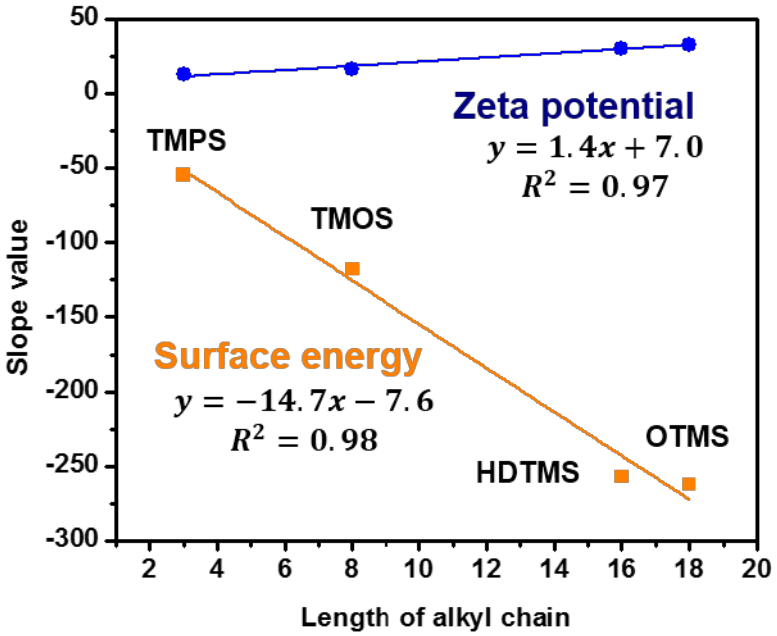

Fig. 6 Correlation between the slope of fitting lines (Fig. 5) and carbon number in the alkyl chain of different silanes.

Besides the linear relationship among the surface properties of each silane in Fig. 5, it is also found that the slope of the fitting lines changes monotonously with increasing silane alkyl chain carbon number. The correlation between the slope of the fitting lines (both surface energy and zeta potential) and alkyl chain carbon number of different silanes is plotted in Fig. 6. Surprisingly, highly linear relationship with correlation factor of $R^2 \geq 0.97$ was found across different silanes. This linear relationship is definitely useful to predict the slope of fitting lines of other silane molecules with C3-C18 alkyl tail chains. It is also worth noticing that the intercept of the fitting lines (both grafting density vs. surface energy; grafting density vs. surface potential) in Fig. 5 are very close to each other. Therefore, the linear prediction model was constructed by taking the calculated slope and average intercept. According to two linear regression formulas in Fig. 6, the following two equations (3) and (4) can be derived to predict silane grafting density (N_s') and surface energy (G'):

$$N_s' = \frac{Z+32.1}{1.4x+7} \quad (3)$$

$$G' = -(14.7x + 7.6)N_s' + 93.5 \quad (4)$$

where x is the alkyl chain carbon number of specific silane molecules and Z is the measured zeta potential. To test the validity of these two derived formulas, another set of silica samples modified with different silanes were prepared and named TMPS-6, TMOS-6, HDTMS-6 and OTMS-6. By measuring the zeta potential (Z) of these silica particles and inputting the carbon number (x), N_s' and G' could be calculated from equations (3) and (4), respectively. Detailed calculation results on grafting density and surface energy of these four samples are summarized in Table 4. Meanwhile, TGA and contact angle measurements were conducted to quantify the silane grafting density and surface energy, respectively. The error percentage between prediction model calculation and experimental measurement is mostly around 10% except HDTMS-6. Therefore, this model could serve as a useful tool to quickly predict silane grafting density and surface energy by simple and fast zeta potential measurement.

Table 4. Comparison of calculated and measured results.

Sample	Calculated value				Measured value				Error	
	Z **/mV**	***Ns'*** **/nm²**	***G'*** **/mN·m⁻¹**	***Δm*** **/%**	θ_{water}	θ_{EG}	***Ns*** **/nm²**	***G*** **/mN·m⁻¹**	***Ns*** **/%**	***G*** **/%**
TMPS-6	-20.5	1.04	40.0	2.1	84.0	49.4	0.94	35.8	9.7	11.5
TMOS-6	-23.2	0.49	32.3	2.4	101.4	56.4	0.45	30.2	8.7	6.9
HDTMS-6	-25.9	0.21	42.3	2.1	83.3	46.3	0.18	38.2	17.2	10.7
OTMS-6	-22.8	0.29	14.9	3.3	114.2	38.8	0.31	16.2	7.9	8.1

4. Conclusion

Microscopic silane grafting density and macroscopic surface properties has been linked in silica nanoparticles grafted with four different alkyl chain terminated silanes

(TMPS, TMOS, HDTMS and OTMS). By successful control of silane grafting density, linear relationships of grafting density vs. surface energy and grafting density vs. surface potential have been explored in silane-grafted silica. Moreover, based on the slope of the fitting lines from four selected silanes, a linear prediction model can be built to correlate fitting line slope and alkyl chain carbon number and then to be used to predict surface property of silica grafted by other silanes with similar alkyl chain terminated groups. Using all the collected surface information, a prediction model has been built to calculate silane grafting density on silica surface and surface energy of the modified silica by taking surface potential and alkyl chain carbon number as inputs. This method provides a quick access to silica surface property by simple, fast and convenient surface potential measurement.

Acknowledge

The authors are grateful to NSF Center for Tire Research (CenTiRe) for its support and National Science Foundation Research Experiences for Undergraduates grant (IIP-1160982).

References

1. Liz-Marzán, L. M.; Giersig, M.; Mulvaney, P. Synthesis of nanosized gold-silica core-shell particles. *Langmuir* **1996,** *12* (18), 4329-4335.

2. Kapgate, B. P.; Das, C.; Basu, D.; Das, A.; Heinrich, G. Rubber composites based on silane-treated stober silica and nitrile rubber: Interaction of treated silica with rubber matrix. *Journal of Elastomers and Plastics* **2015,** *47* (3), 248-261.

3. Dohi, H.; Horiuchi, S. Locating a silane coupling agent in silica-filled rubber composites by EFTEM. *Langmuir* **2007,** *23* (24), 12344-12349.

4. Coffman, E. A.; Melechko, A. V.; Allison, D. P.; Simpson, M. L.; Doktycz, M. J. Surface patterning of silica nanostructures using bio-inspired templates and directed synthesis. *Langmuir* **2004,** *20* (20), 8431-8436.

5. Slowing, I. I.; Vivero-Escoto, J. L.; Wu, C.-W.; Lin, V. S.-Y. Mesoporous silica nanoparticles as controlled release drug delivery and gene transfection carriers. *Advanced drug delivery reviews* **2008,** *60* (11), 1278-1288.

6. Minakuchi, H.; Nakanishi, K.; Soga, N.; Ishizuka, N.; Tanaka, N. Octadecylsilylated porous silica rods as separation media for reversed-phase liquid chromatography. *Analytical chemistry* **1996,** *68* (19), 3498-3501.

7. Vashist, S. K.; Lam, E.; Hrapovic, S.; Male, K. B.; Luong, J. H. Immobilization of antibodies and enzymes on 3-aminopropyltriethoxysilane-functionalized bioanalytical platforms for biosensors and diagnostics. *Chemical reviews* **2014,** *114* (21), 11083-11130.

8. Khayet, M.; Villaluenga, J. P. G.; Valentin, J. L.; López-Manchado, M. A.; Mengual, J. I.; Seoane, B. Filled poly(2,6-dimethyl-1,4-phenylene oxide) dense membranes by silica and silane modified silica nanoparticles: characterization and application in pervaporation. *Polymer* **2005,** *46* (23), 9881-9891.

9. Frickel, N.; Messing, R.; Gelbrich, T.; Schmidt, A. M. Functional Silanes as Surface Modifying Primers for the Preparation of Highly Stable and Well-Defined Magnetic Polymer Hybrids. *Langmuir* **2010,** *26* (4), 2839-2846.

10. Bravo, J.; Zhai, L.; Wu, Z.; Cohen, R. E.; Rubner, M. F. Transparent Superhydrophobic Films Based on Silica Nanoparticles. *Langmuir* **2007,** *23* (13), 7293-7298.

11. Ji, T.; Li, L.; Wang, M.; Yang, Z.; Lu, X. Carbon-protected Au nanoparticles supported on mesoporous TiO 2 for catalytic reduction of p-nitrophenol. *RSC Advances* **2014,** *4* (56), 29591-29594.

12. Howarter, J. A.; Youngblood, J. P. Optimization of silica silanization by 3-aminopropyltriethoxysilane. *Langmuir* **2006,** *22* (26), 11142-11147.

13. Perrin, A.; Lanet, V.; Theretz, A. Quantification of specific immunological reactions by atomic force microscopy. *Langmuir* **1997,** *13* (9), 2557-2563.

14. Mangos, D. N.; Nakanishi, T.; Lewis, D. A. A simple method for the quantification of molecular decorations on silica particles. *Science and Technology of Advanced Materials* **2014,** *15* (1), 015002.

15. Foda, M. F.; Huang, L.; Shao, F.; Han, H.-Y. Biocompatible and highly luminescent near-infrared CuInS2/ZnS quantum dots embedded silica beads for cancer cell imaging. *ACS applied materials & interfaces* **2014,** *6* (3), 2011-2017.

16. Fischer, T.; Dietrich, P. M.; Streeck, C.; Ray, S.; Nutsch, A.; Shard, A.; Beckhoff, B.; Unger, W. E. S.; Rurack, K. Quantification of Variable Functional-Group Densities of Mixed-Silane Monolayers on Surfaces via a Dual-Mode Fluorescence and XPS Label. *Analytical Chemistry* **2015,** *87* (5), 2685-2692.

17. Castellano, M.; Marsano, E.; Turturro, A.; Conzatti, L.; Busca, G. Dependence of surface properties of silylated silica on the length of silane arms. *Adsorption-Journal of*

the International Adsorption Society **2012,** *18* (3-4), 307-320.

18. Jesionowski, T.; Krysztafkiewicz, A. Influence of silane coupling agents on surface properties of precipitated silicas. *Applied Surface Science* **2001,** *172* (1-2), 18-32.

19. Norrman, K.; Papra, A.; Kamounah, F. S.; Gadegaard, N.; Larsen, N. B. Quantification of grafted poly(ethylene glycol)-silanes on silicon by time-of-flight secondary ion mass spectrometry. *Journal of Mass Spectrometry* **2002,** *37* (7), 699-708.

20. Liu, X.; Thomason, J. L.; Jones, F. R. XPS and AFM study of interaction of organosilane and sizing with E-glass fibre surface. *The Journal of Adhesion* **2008,** *84* (4), 322-338.

21. Rostami, M.; Mohseni, M.; Ranjbar, Z. An attempt to quantitatively predict the interfacial adhesion of differently surface treated nanosilicas in a polyurethane coating matrix using tensile strength and DMTA analysis. *International Journal of Adhesion and Adhesives* **2012,** *34*, 24-31.

22. Castellano, M.; Turturro, A.; Marsano, E.; Conzatti, L.; Vicini, S. Hydrophobation of silica surface by silylation with new organo-silanes bearing a polybutadiene oligomer tail. *Polymer Composites* **2014,** *35* (8), 1603-1613.

23. Freire, J. M.; Domingues, M. M.; Matos, J.; Melo, M. N.; Veiga, A. S.; Santos, N. C.; Castanho, M. A. Using zeta-potential measurements to quantify peptide partition to lipid membranes. *European Biophysics Journal* **2011,** *40* (4), 481-487.

24. Ji, T.; Chen, L.; Schmitz, M.; Bao, F. S.; Zhu, J. Hierarchical macrotube/mesopore carbon decorated with mono-dispersed Ag nanoparticles as a highly active catalyst. *Green Chemistry* **2015,** *17* (4), 2515-2523.

25. Sing, K.; Williams, R. Physisorption hysteresis loops and the characterization of nanoporous materials. *Adsorption Science & Technology* **2004,** *22* (10), 773-782.

26. Villegas, M.; Navarro, J. F. Characterization of B2O3-SiO2 glasses prepared via sol-gel. *Journal of materials science* **1988,** *23* (7), 2464-2478.

27. Yang, H.; Li, F.; Shan, C.; Han, D.; Zhang, Q.; Niu, L.; Ivaska, A. Covalent functionalization of chemically converted graphene sheets via silane and its reinforcement. *Journal of Materials Chemistry* **2009,** *19* (26), 4632-4638.

28. Zhuravlev, L.; Potapov, V. Density of silanol groups on the surface of silica precipitated from a hydrothermal solution. *Russian Journal of Physical Chemistry A, Focus on Chemistry* **2006,** *80* (7), 1119-1128.

29. Jeong, D. S.; Hong, C. K.; Lim, G. T.; Seo, G.; Ryu, C. S. Networked silica with exceptional reinforcing performance for SBR compounds: interconnected by Methylene Diphenyl Diisocyanate. *Journal of Elastomers and Plastics* **2009,** *41* (4), 353-368.

30. Araźna, A.; Kozioł, G.; Janeczek, K.; Futera, K.; Stęplewski, W. Investigation of surface properties of treated ITO substrates for organic light-emitting devices. *Journal of Materials Science: Materials in Electronics* **2013,** *24* (1), 267-271.

31. Ramier, J.; Chazeau, L.; Gauthier, C.; Guy, L.; Bouchereau, M. N. Grafting of silica during the processing of silica-filled SBR: Comparison between length and content of the silane. *Journal of Polymer Science Part B-Polymer Physics* **2006,** *44* (1), 143-152.

32. Salgın, S.; Salgın, U.; Bahadır, S. Zeta potentials and isoelectric points of biomolecules: the effects of ion types and ionic strengths. *Int. J. Electrochem. Sci* **2012,**

7, 12404-12414.

33. Ukaji, E.; Furusawa, T.; Sato, M.; Suzuki, N. The effect of surface modification with silane coupling agent on suppressing the photo-catalytic activity of fine TiO 2 particles as inorganic UV filter. *Applied Surface Science* **2007,** *254* (2), 563-569.